Sciencexpress Report

Character and Spatial Distribution of OH/H_2O on the Surface of the Moon Seen by M^3 on Chandrayaan-1

C. M. Pieters,[1]* J. N. Goswami,[2,3] R. N. Clark,[4] M. Annadurai,[3] J. Boardman,[5] B. Buratti,[6] J.-P. Combe,[7] M. D. Dyar,[8] R. Green,[6] J. W. Head,[1] C. Hibbitts,[9] M. Hicks,[6] P. Isaacson,[1] R. Klima,[1] G. Kramer,[7] S. Kumar,[10] E. Livo,[4] S. Lundeen,[6] E. Malaret,[11] T. McCord,[7] J. Mustard,[1] J. Nettles,[1] N. Petro,[12] C. Runyon,[13] M. Staid,[14] J. Sunshine,[15] L. A. Taylor,[16] S. Tompkins,[17] P. Varanasi[6]

[1]Brown University, Providence, RI 02912, USA. [2]Physical Research Laboratory, Ahmedabad, India. [3]Indian Space Research Organization, Bangalore, India. [4]U.S. Geological Survey, Denver, CO 80225, USA. [5]Analytical Imaging and Geophysics, Boulder, CO 80303, USA. [6]Jet Propulsion Laboratory, Pasadena, CA 91109, USA. [7]Bear Fight Center, Winthrop, WA 98862, USA. [8]Mt. Holyoke College, South Hadley, MA 01075, USA. [9]Applied Physics Laboratory, Laurel, MD 20723–6005, USA. [10]National Remote Sensing Agency, Hyderabad, India. [11]Applied Coherent Technology Corporation, Herndon, VA 22070, USA. [12]NASA Goddard, Greenbelt, MD 20771, USA. [13]College of Charleston, Charleston, SC 29424, USA. [14]Planetary Science Institute, Tucson, AZ 85719–2395, USA. [15]University of Maryland, College Park, MD 20742, USA. [16]University of Tennessee, Knoxville, TN 37996–1410, USA. [17]Defense Advanced Research Projects Agency, Arlington, VA 22203, USA.

*To whom correspondence should be addressed. E-mail: carle_pieters@brown.edu

The search for water on the surface of the anhydrous Moon remained an unfulfilled quest for 40 years. The Moon Mineralogy Mapper (M^3) on Chandrayaan-1 has now detected absorption features near 2.8 to 3.0 μm on the surface of the Moon. For silicate bodies, such features are typically attributed to OH- and/or H_2O-bearing materials. On the Moon, the feature is seen as a widely distributed absorption that appears strongest at cooler high latitudes and at several fresh feldspathic craters. The general lack of correlation of this feature in sunlit M^3 data with neutron spectrometer H abundance data suggests that the formation and retention of OH and H_2O is an ongoing surficial process. OH/H_2O production processes may feed polar cold traps and make the lunar regolith a candidate source of volatiles for human exploration.

The Moon has been believed to be quite dry since the return of lunar samples from the Apollo and Luna programs. Many Apollo samples contain some trace water or minor hydrous minerals, but these have typically been attributed to terrestrial contamination (see supporting online material text). A possible accumulation of volatiles, including water frost and ice, in the permanently shadowed regions of the lunar poles has nevertheless been discussed for decades (*1*–*3*). The Lunar Prospector neutron spectrometer directly measured H over the Moon and found a higher abundance associated with the permanently shadowed regions of both poles (*4*, *5*), implying that the lunar poles could be potential cold traps for volatiles (*6*), some of which could be linked to solar-wind hydrogen (*7*). Here we present measurements acquired by The Moon Mineralogy Mapper (M^3) [see (*8*)], a NASA instrument on Chandrayaan-1, India's first mission to the Moon, that show small amounts of OH/H_2O on the uppermost surface of the Moon.

The M^3 spectrometer measures visible and near-infrared wavelengths, which contain highly diagnostic absorptions due to minerals as well as OH and H_2O (*9*) (fig. S1). Absorptions occur as solar radiation passes through multiple randomly oriented particles in the upper 1 to 2 mm of soil; reflectance spectra exhibit these combined absorptions from all particles. As soils evolve in the lunar environment, individual grains develop silicate glass coatings that contain nano-phase metallic iron ($npFe^0$) (*10*–*12*). The cumulative abundance of this weathering-derived $npFe^0$ substantially decreases the measured strength of all absorption bands of lunar material, especially for soils from the FeO-rich maria (*13*).

We have evaluated the 3-μm spectral region in current M^3 data over the sunlit portion of the Moon to search for evidence of water. A feature near 3 μm was seen in several areas of the first returned sequences of M^3 data. As global data accumulated (Fig. 1), it became evident that this feature is observed systematically across the Moon. For various illumination geometries, the strength of the absorption feature near 3 μm (Fig. 1B) is computed as a relative band depth = 1 – (Rb/Rc), where Rb = average of channels at 2896 and 2936 nm, and Rc is the approximate continuum, given by the average of channels at 2617, 2657, and 2697 nm. A small component of emitted thermal radiation often occurs along with reflected solar radiation in M^3 radiance measurements. When the surface is warm (greater than ~250 to 300 K), this added component is evident at wavelengths longer than 2000 nm. An iterative procedure to measure and remove this

thermal emission component has been developed for M^3 data (*14*). Surface temperature derived from the M^3 measurements are illustrated in Fig. 1C. As these M^3 measurements progressed across the lunar surface, solar illumination angle gradually decreased from east to west. For higher-temperature equatorial mare regions, the added thermal radiation could be up to 30% of the signal received at 3 μm. Minor thermal emission may hide the presence of a weak absorption feature near 3 μm, and although the relative band-depth image (Fig. 1B) excludes areas with detectible thermal radiation, it is a conservative limit to the distribution of the feature [see (*8*)].

Although it is impossible to capture the full range of lunar surface mineralogy with three parameters, specific mineral properties displayed in red, green, and blue in Fig. 1D are directly linked to our understanding of the diagnostic absorptions of lunar materials (*9*, *15*). Most importantly, these mineral patterns (which rely on spectral channels from the visible through ~2600 nm) do not appear to be correlated with M^3 measurements at slightly longer wavelengths (Fig. 1, B and C).

At the spatial resolution of these initial M^3 data (140 m/pixel), the 3-μm feature is identified for soils at moderate to high latitudes (Fig. 1B) as well as at several fresh (plagioclase-rich) impact craters. In the highlands, small (<1 km) morphologically fresh impact craters have ejecta patterns with a prominent 3-μm feature relative to their surroundings (fig. S2). More than one specific absorption may account for the spectral feature, and/or the distribution of the absorption appears variable with local conditions (effects of temperature, solar illumination). For example, Ryder Crater, a fresh ~17-km Copernican-aged crater on the lunar farside (Fig. 2) and its immediate ejecta exhibit no discernable thermal emission component in M^3 data. Although most of the crater exposes plagioclase-rich rocks, it is heterogeneous and contains regions with small amounts of Fe-bearing minerals (Fig. 2E). An enhanced 3-μm band is seen in distal Ryder ejecta to the northwest. A diffuse and approximately inverse correlation of 3-μm band strength with measured signal brightness is seen across the scene, and suggests sensitivity either to solar-wind ions or to solar insolation (i.e., small local variations of emissivity or other thermal effects). The traverse around the sunlit rim of Ryder Crater illustrates this observation (see also fig. S3).

Individual M^3 spectra focusing on the 2000- to 3000-nm part of the spectral range acquired from highland terrain just east of the central meridian of the lunar nearside suggest that the relative strength of the 3-μm feature increases with latitude (Fig. 3A). These spectra are derived from a current radiance calibration (version K) and with modest image-based band-to-band calibrations with no thermal emission correction applied. Example spectra of several forms of H_2O and OH that might be seen with remote detectors are shown for comparison (Fig. 3B). The pattern seen in M^3 data may indicate increasingly strong OH/H_2O absorptions with latitude, but we cannot eliminate the possibility that a 3-μm feature is present at lower latitudes but is masked by a minor thermal emission component beyond 2.6 μm (*8*).

We implemented several tests to validate the M^3 results for the 3-μm region. We first scrutinized pre-flight laboratory calibrations of M^3 obtained at lunar operating temperatures and in a vacuum [see (*16*)]. Initial atmospheric effects were readily identified as the instrument reached vacuum equilibrium. Calibration data for two independent standards [spectralon, infragold (*17*)] were acquired. When applied to M^3 in-flight data, they produce results that do not significantly alter the presence of the observed 3-μm feature, but do alter its shape. We use the infragold standard because the spectralon has a weak feature near 2.8 μm. Furthermore, using purely in-flight image-based methods that are independent of terrestrial laboratory calibration approaches, a feature near 3 μm is seen in contrasting relative reflectance spectra.

At moderately high latitudes, there is sufficient orbit-to-orbit overlap that M^3 made repeat measurements of the same area on the lunar surface 2 hours apart under approximately the same illumination. The characteristics of observed spectral features were identical within data precision. Every month Chandrayaan-1 passes the same location on the surface, but with a ~30° change in solar illumination angle at the equator. We identified and processed four pairs of image strips across the western portion of the Orientale Basin on the farside western limb that have nearly identical spatial coverage, but substantially different illumination conditions. A local morning set was acquired in February 2009 and the second set was acquired two months later in local afternoon. For several weeks between these optical periods, M^3 activated a decontamination heater to drive off any condensed volatiles. Typical results are shown in Fig. 4, which is a region (~53°S , 259°E) that is low enough in temperature to exhibit no discernable thermal emission for sunlit areas in either geometry. Because of the large variations in local brightness, the spectra are scaled relative to an area exhibiting the weakest 3-μm absorption. The presence of the 3-μm feature was repeatable, but the time of lunar day does affect the apparent distribution and strength of the absorption.

Lastly, two independent spacecraft with spectrometers that extend beyond 3-μm, Cassini in 1999 and Deep Impact in June 2009, have flown by the Moon for calibration purposes, and recent analysis of these data confirmed the presence of absorptions in spectra of the lunar surface similar to those reported here (*18*, *19*). Because these spectrometers extend farther into the near-infrared than M^3, they are able to more fully characterize the shape of the 3-μm absorption, which is

important information to constrain the nature of the absorbing species.

Approximate abundance estimates of OH or H_2O are only possible using specific model assumptions about the physical form and location of the hydrated species. As one example, simple attenuation according to Beer's law might be assumed for a case where the detected water/ion is a surficial deposit on individual regolith grains, with the observed reflectance of the regolith dominated by sunlight absorbed and scattered by the grains themselves. Modeled abundance could be as high as 770 ppm (*20*), but is dependent on particle size, and the total abundance of hydrated material in the bulk upper regolith would be substantially smaller if hydration is not retained during regolith gardening.

The 3-μm feature measured by M^3 originates from the upper few mm of the surface, whereas the bulk H detected by the Lunar Prospector neutron spectrometer (LP-NS) (*21*–*23*), represents the upper ~50 cm of the regolith. Because the spatial resolution of the LP-NS is 2-3 orders of magnitude lower than that of M^3, only broad features on the order of hundreds of km can be compared directly outside the permanently shadowed regions. Two distinct differences are noted. In contrast to that seen for M^3, the generally diffuse nature of LP-NS H for most regions on the Moon shows no pattern of significant H present at high latitudes near the poles (<80°). Furthermore, some of the lowest regional abundance of LP-NS H corresponds to large expanses of anorthositic or freshly disturbed (immature) highland material (*21*, *22*). One such example covered by both M^3 and LP-NS is the 113 km diameter crater Goldschmidt (73.0°N, 3.8°W) and its smaller fresh companion, the 51 km diameter Anaxagoras (73.4°N, 10.1°W). As in M^3 observations of many smaller feldspathic craters, M^3 data for Goldschmidt exhibit a prominent 3-μm absorption (Fig. 1B) whereas in LP-NS data the region exhibits a distinctly low H abundance [see fig. S4 and (*23*)], suggesting the hydrated materials observed by M^3 does not occur at depth.

The M^3 3-μm data clearly indicate that a minor hydrated phase or hydration process occurs on the lunar surface. This finding could imply that the Moon contains primary hydrated mineral phases that are uncommon in the limited Apollo, Luna, and lunar meteorite collections. These unsampled phases might be endogenic to the Moon and freshly exposed by craters in ancient highland terrain, or they may form during an impact event by a water-bearing comet or asteroid. On the other hand, H_2O and OH species might also be continuously created when solar-wind protons (H^+) interact with the oxygen-rich surfaces during the formation of lunar soil particles. In addition, fresh broken surfaces and soil grains may readily react with protons from the solar-wind forming strong surficial OH bonds. Either of these may be highly dependent on the temperature and solar illumination environment. The differences described between LP-NS H abundance and M^3 3-μm band-depth (linked to OH/H_2O abundance) imply that the M^3 detection of OH/H_2O species is distinctly surface-correlated, i.e., linked to the upper few millimeters of the lunar regolith, but not significantly deeper. Thus, surficial processes involving the solar-wind are the most likely explanation of our observations.

The process for producing OH/H_2O on the Moon may provide an ongoing mechanism for delivery of these volatile elements to cold traps in the polar permanently shadowed regions. Perhaps most importantly, harvesting the lunar regolith for volatiles now becomes a serious option for long-term human activities.

References and Notes

1. H. C. Urey, *The Planets: Their Origin and Development* (Yale Univ. Press, New Haven, CT, 1952).
2. K. Watson, B. C. Murray, H. Brown, *J. Geophys. Res.*, **66**, 3033 (1961).
3. J. R. Arnold, *J. Geophys. Res.* **84**, 5659 (1979).
4. W. C. Feldman *et al*., *Science* **281**, 1496 (1998).
5. W. C. Feldman *et al*., *J. Geophys. Res.* **106**, 23231, (2001).
6. D. H. Crider, R. R. Vondrak, *Adv. Space Res.* **30**, 1869 (2002).
7. L. Starukhina, Y. Shkuratov, *Icarus* **147**, 585 (2000).
8. Materials and methods are available as supporting material on *Science* Online.
9. R. G. Burns, *Mineralogical Applications of Crystal Field Theory* (Cambridge Univ. Press, ed. 2, 1993).
10. L. P. Keller, D. S. McKay, *Geochim. Cosmochim. Acta* **61**, 2331 (1997).
11. S. K. Noble, C. M. Pieters, L. P. Keller, *Icarus* **192**, 629 (2007).
12. L. A. Taylor, C. M. Pieters, L. P. Keller, R. V. Morris, D. S. McKay, *J. Geophys. Res.* **106**, 27985 (2001).
13. C. M. Pieters *et al*., *Meteorit. Planet. Sci.* **35**, 1101 (2000).
14. We have used the approach described in R. N. Clark, *Icarus*, **40**, 94 (1979). Briefly, our thermal removal algorithm estimates the thermal emission as an excess signal compared to a value derived from the reflectance trend of unaffected shorter wavelengths. The thermal emission component includes an estimate of emissivity and our procedure cannot artificially create the appearance of an absorption feature. See also (*8*).
15. Bright feldspathic (highland) soils are relatively red and the dark mafic-rich maria contain little of this component. The green and the blue displayed channels (green-cyan-blue colors in Fig. 3D) capture the relative band strength of diagnostic absorptions of several ferrous minerals. Regions containing abundant and diverse mafic minerals are highlighted by these two parameters. Both are calculated relative to a continuum and are integrated

across M^3 channels within the broad mineral absorption bands (see fig. S1). The strength of these particular parameters is largely sensitive to the relative abundance of pyroxene, but the integrated 1000 nm band-strength parameter (green) is also sensitive to other mafic minerals present (e.g., olivine). The band-strengths of all absorptions are modulated by the abundance of opaque phases (ilmenite, chromite) and $npFe^0$

16. R. O. Green *et al*., 40th Lunar and Planetary Science Conference, Houston #2307 (2009).
17. The reflectance standards used in the calibration of M^3 are 12 × 12 inch panels of Spectralon SN: 50119-1-1 and Infragold SN: 50205-1-1 from Labsphere Inc.
18. R. N. Clark, *Science*; published online 24 September 2009 (10.1126/science.1178105).
19. J. S. Sunshine, *et al*., *Science*; published online 24 September 2009 (10.1126/science. 1179788).
20. A measured depth of the 3-μm absorption band of ~7% would be equivalent to an effective thickness of such surficial water of ~0.09 μm, which could be accounted for by a single or few molecular layers of water/ion on individual grains given an effective particle size for the interacting upper lunar regolith of ~1 μm and an overall optical depth of ~300 μm. A monolayer of water/ion would not tend to migrate into the grains, which would therefore remain dry—i.e., the overall abundance of water in the surface would remain low, but potentially stable. If this surficial water/ion were photolytically dissociated, the resulting H ions may simply migrate along the surface until interacting with another O atom in the grain to again form OH or H_2O resulting in an effective pseudo-stability or temporary steady-state. If the regolith grains are anorthostic plagioclase, a monolayer of water on a 1-μm spherical grain would equate to a molar abundance of 0.6%, and ~770-ppm mass fraction, given a 1:1 ratio of water molecule/ion to the anorthositic surface molecules. However, if the effective particle size of regolith grains carrying the water is larger than 1 μm, then the surface water proportion will be less.
21. J. R. Johnson *et al*., *J. Geophys. Res.*, **107**, 10.1029/2000JE001430 (2002).
22. S. Maurice, D. J. Lawrence, W. C. Feldman, R. C. Elphic, O. Gasnault *J. Geophys. Res.*, **109**, E07S04,10.1029/2003JE002208 (2004).
23. D. J. Lawrence *et al*., *J. Geophys. Res.* **111**, E08001, 10.1029/2005JE002637 (2006).
24. J. W. Boardman *et al*., 6th EARSeL SIG IS workshop on Imaging Spectroscopy, Tel Aviv, Israel (2009).
25. Apparent reflectance is radiance at sensor multiplied by pi and divided by a solar distance-normalized solar spectrum. Currently M^3 often also uses a cos(i) scalar for simple photometric approximations, where i is the solar incidence angle relative to a smooth sphere.
26. D. M. Wieliczka, S. Weng, M. T. Querry, *Appl. Opt.* **28**, 1714 (1989).
27. S. G. Warren, *Appl. Opt.* **23**, 1206 (1984).
28. S. J. Seaman, M. D. Dyar, N. Marinkovic, N. Dunbar, *Amer. Mineral* **91**, 12 (2006).
29. M^3 is funded as a Mission of Opportunity under NASA's Discovery program contract NNM05AB26C to Brown University. Lunar reflectance spectra were acquired using the NASA/Keck RELAB, a multiuser facility supported by NASA grant NNG06GJ31G. A portion of this research was carried out at the Jet Propulsion Laboratory, California Institute of Technology, under a contract with the National Aeronautics and Space Administration. We thank the team of engineers at JPL who designed and built M^3 (led by T. Glavich and M. White) and the Chandrayaan-1 mission operations team (led by N. S. Hegde, with M^3 implementation largely by S. Gomathi) whose mission support has made M^3 data possible. The M^3 team is honored to be a guest instrument on India's first mission to the Moon.

Supporting Online Material

www.sciencemag.org/cgi/content/full/1178658/DC1
Materials and Methods
SOM Text
Figs. S1 to S5
References

5 July 2009; accepted 15 September 2009
Published online 24 September 2009;
10.1126/science.1178658
Include this information when citing this paper.

Fig. 1. M^3 low-resolution mode data for the lunar nearside acquired from Chandrayaan-1 in a 100-km orbit. All data have been spatially averaged by a factor of 100 and projected to produce a hemispheric overview (*24*). During this period of observations, the illumination geometry at the equator ranges from 45° in the east to 58° on the western limb. (**A**) Reflected light at 750 nm. Surface reflectance has not been adjusted for solar illumination and brightness decreases toward the poles. (**B**) Measured 3-μm absorption strength. Bright represents strong absorption. The large northern crater near 0° longitude with strong 3-μm absorption is Goldschmidt (indicated with arrow). (**C**) Derived surface temperature (240 to 360 K), and (**D**) Color composite designed to illustrate major mineral absorptions (red, reflectance at 1580 nm; green, integrated band depth near 1000 nm; blue, integrated band depth near 2000 nm after thermal removal). In this composite, the feldspathic highlands are largely red (with few mafic minerals) whereas the basaltic maria are variations of green-

cyan-blue illustrating the presence and diversity of mafic minerals.

Fig. 2. Subscene of M^3 strip M3G20090125T172600 including Ryder Crater (on right), centered at 143.2 E longitude and 44.5 S latitude. (**A**) Bightness image at 2856 nm. (**B**) Image of the relative 3-μm feature depth for the same area. A coherent spatial distribution is seen associated with Ryder ejecta as well as a topography related pattern of solar insolation. (**C**) Data cloud for the subscene comparing the relative 3-μm feature depth and near-infrared reflectance. Some regions show a diffuse inverse-correlation as a function of apparent reflectance (*25*). (**D**) Location of spectra collected along the wall of Ryder Crater, from well-illuminated areas (1) to more shaded areas (7 and 8). (**E**) M^3 spectra for the areas shown in (D). Although Ryder Crater exhibits spatially diverse lithologies, the strength of the 3-μm feature is weakest in full sun and increases as solar illumination decreases until the lithology changes (becomes more mafic), a pattern that might be indicative of variations of infilling from minor thermal emission (*8*).

Fig. 3. (**A**) Scaled reflectance spectra for M^3 image strip M3G200902005T150614. All spectra are 7 × 7 pixel averages and no thermal emission has been removed in order to allow the measured flux to be compared. The strongest detected 3-μm feature (~10%) occurs at cool, high latitudes and the measured strength gradually decreases to zero toward mid-latitudes (where thermal emission is necessarily less well constrained by M^3). At lower latitudes (18°) the additional thermal emission component becomes evident at wavelengths above ~2200 nm (*14*). (**B**) Model near-infrared reflectance spectra of H_2O and OH applicable for lunar comparisons. These spectra are highly dependent on physical state. A model of a thin layer of H_2O water (red) and ice (blue) on a 10% reflective surface equivalent to ~1000 ppm abundance is distinct from anorthite (green) and a lunar glass analog (black). Shaded area extends beyond the spectral range of M^3. Calculations are based on optical constants from (*26–28*) assuming no scattering in the H_2O or OH and with a 100-μm path length within the substrate.

Fig. 4. M^3 data taken two months apart during morning (**A**) (OP1) and afternoon (**B**) (OP2) solar illumination. The large 30-km Chadwick Crater is located on the farside at 258.7ºE, 52.7ºS. Spectra in panel (**C**) are scaled reflectance for areas 1 and 2 relative to a local area of strong solar illumination which exhibits a relatively weak 3-μm band in the scene (this reference location varies with geometry). Background soil region 2 (50 × 50 pixels) exhibits a moderately weak and consistent 3-μm band strength. Region 1 within the crater (20 × 20 pixels) exhibits a more prominent apparent band strength, perhaps sensitive to solar illumination. Black boxes (50 × 15 pixels) indicate the reference area selected for spectral ratios.

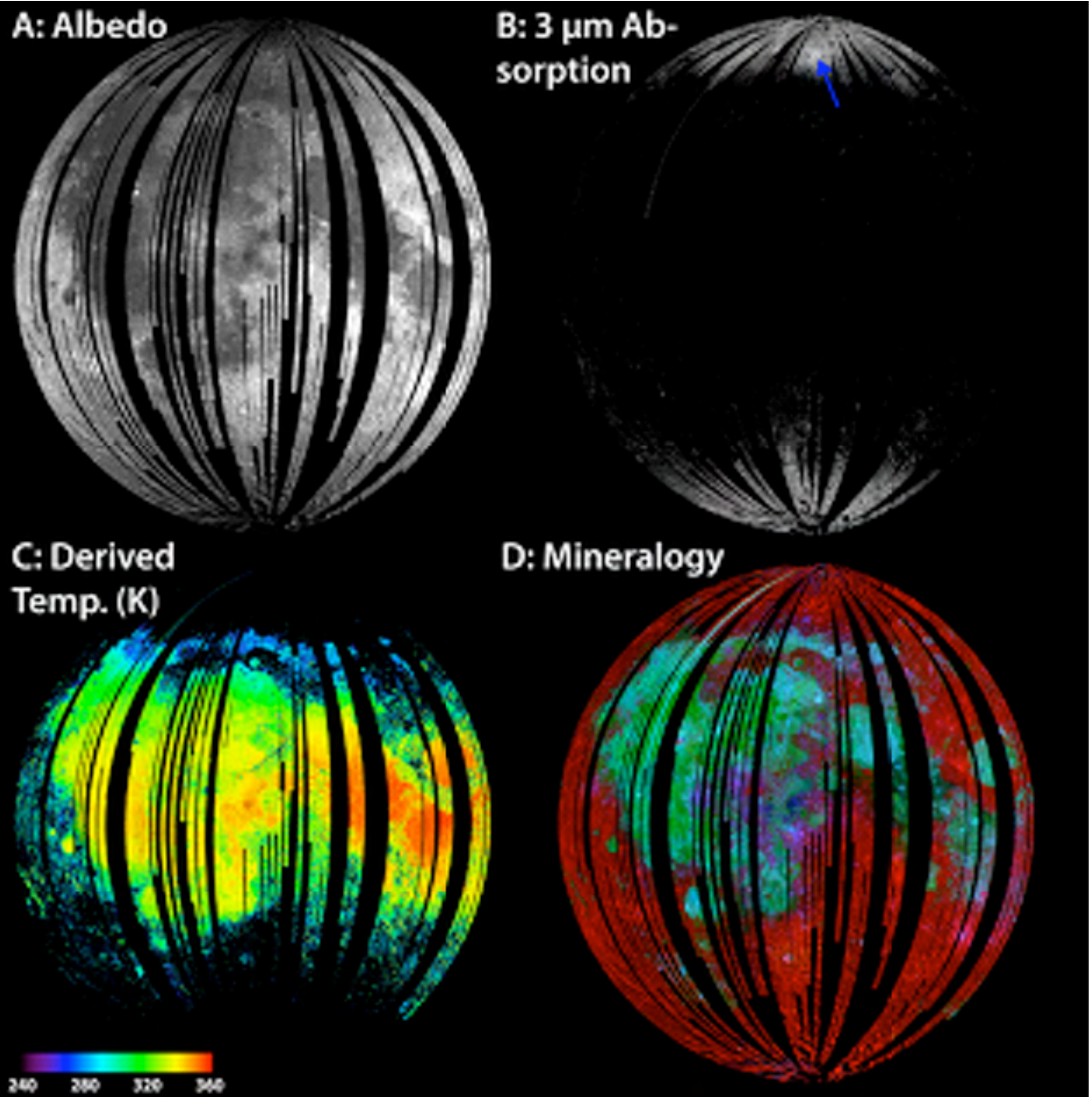
A: Albedo
B: 3 µm Absorption
C: Derived Temp. (K)
D: Mineralogy
240
280
320
360

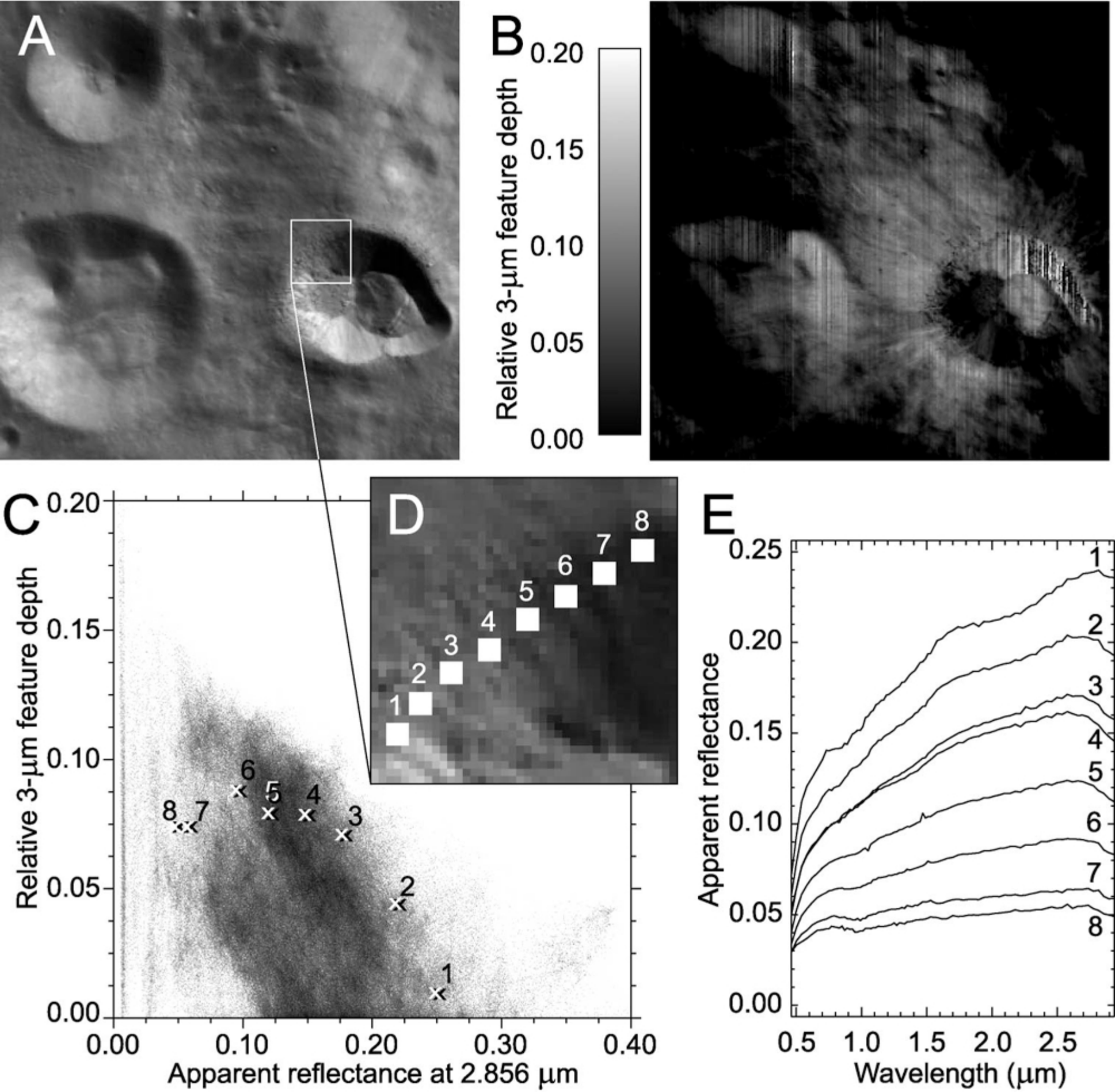
A
B
Relative 3-µm feature depth
0.20
0.15
0.10
0.05
0.00
C
D
E
Relative 3-µm feature depth
Apparent reflectance at 2.856 µm
0.00
0.05
0.10
0.15
0.20
0.30
0.40
Apparent reflectance
Wavelength (µm)
0.25
0.5
1.0
1.5
2.0
2.5
1
2
3
4
5
6
7
8

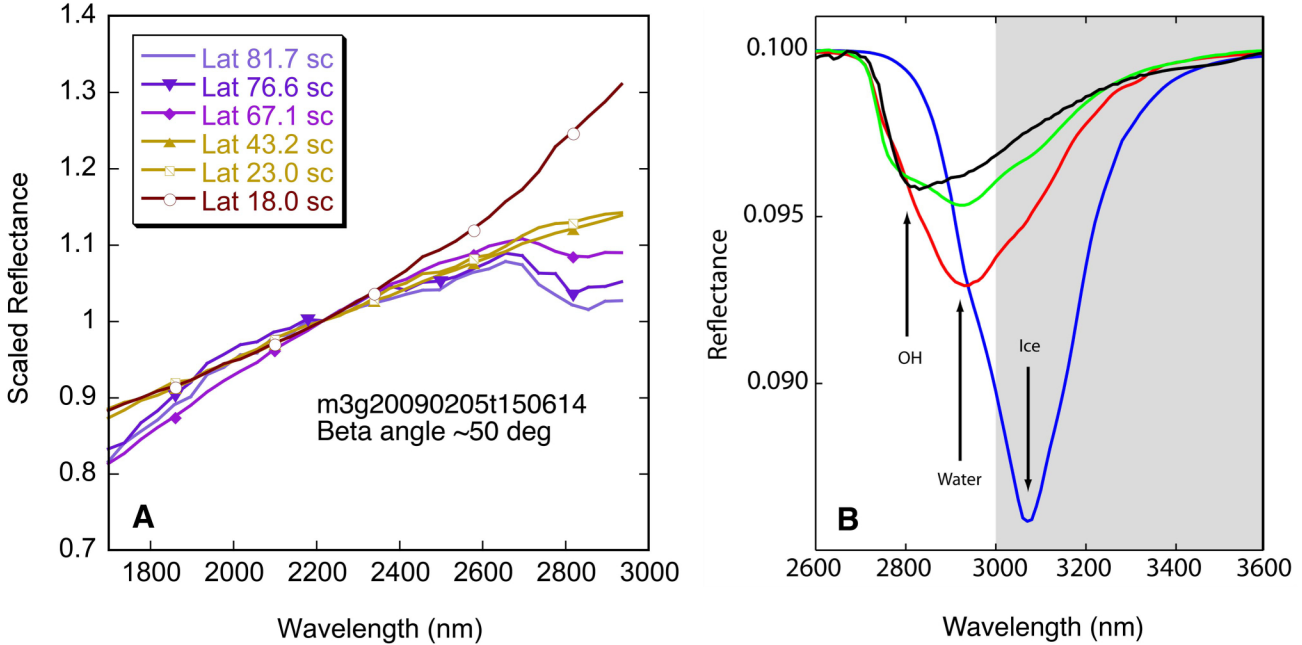
Lat 81.7 sc
Lat 76.6 sc
Lat 67.1 sc
Lat 43.2 sc
Lat 23.0 sc
Lat 18.0 sc
Scaled Reflectance
Wavelength (nm)
m3g20090205t150614
Beta angle ~50 deg
A
Reflectance
OH
Water
Ice
B
Wavelength (nm)

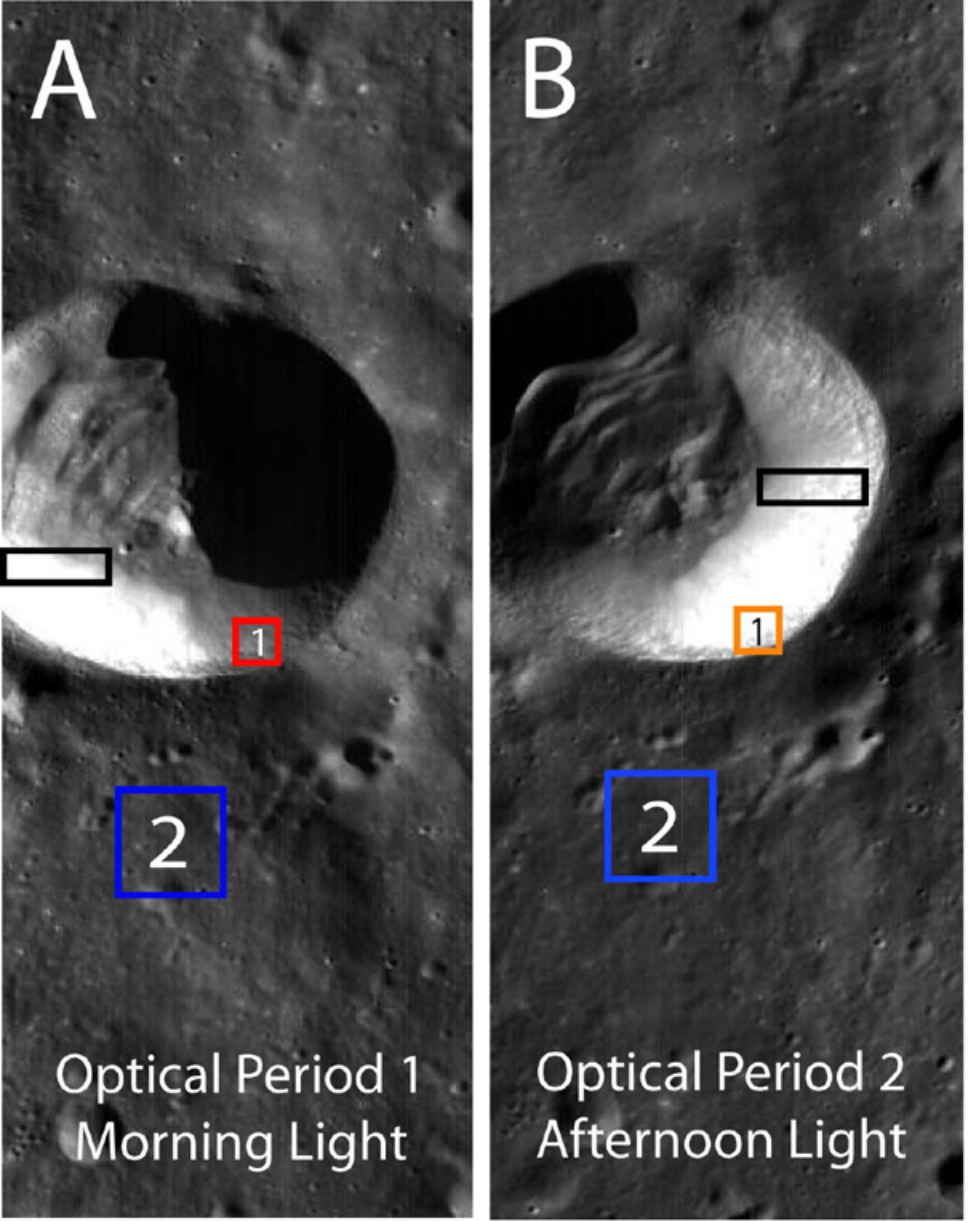
A
1
2
Optical Period 1
Morning Light

B
1
2
Optical Period 2
Afternoon Light

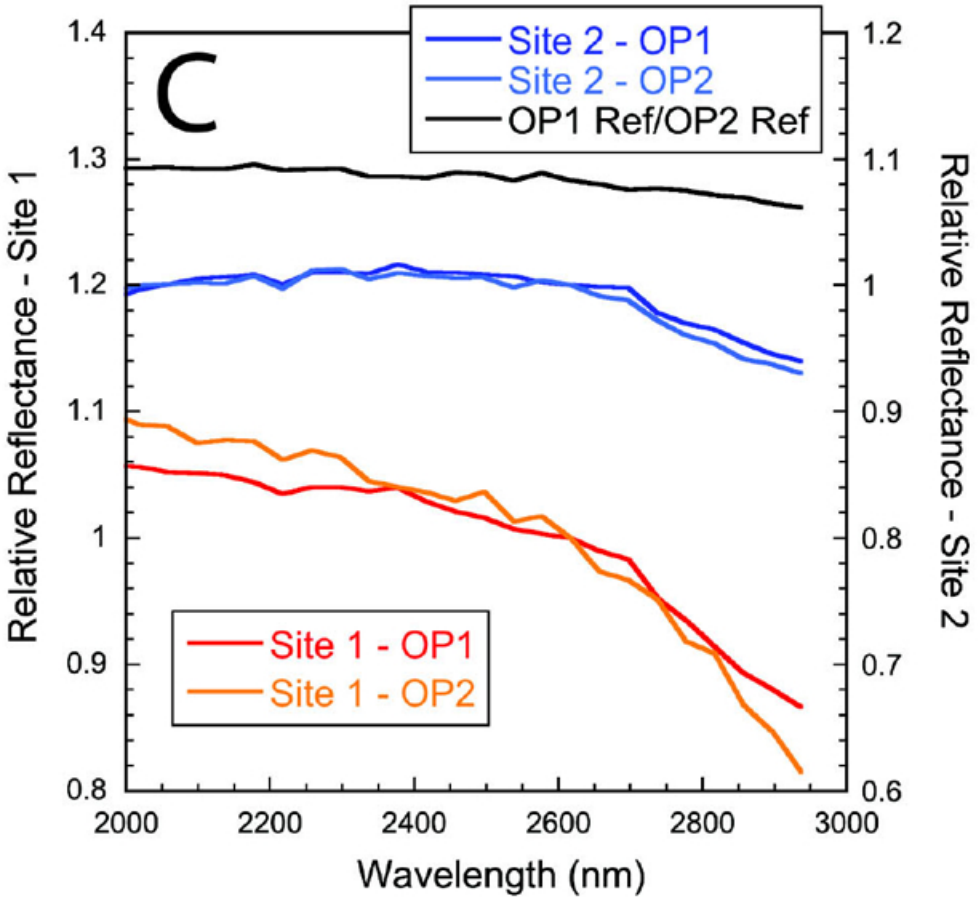
C
Site 2 - OP1
Site 2 - OP2
OP1 Ref/OP2 Ref
Site 1 - OP1
Site 1 - OP2
Relative Reflectance - Site 1
Relative Reflectance - Site 2
Wavelength (nm)
1.4
1.3
1.2
1.1
1
0.9
0.8
1.2
1.1
1
0.9
0.8
0.7
0.6
2000
2200
2400
2600
2800
3000